A MESH MORPHING BASED TECHNIQUE TO EFFICIENTLY PERFORM FSI ANALYSES FOR AEROELASTIC DESIGN APPLICATIONS

M. E. Biancolini[1*], C. Groth[1], E. Costa[2] and F. Lagasco[2]

[1] University of Rome Tor Vergata, Department of Enterprise Engineering, 00100 – Rome

[2] D'Appolonia S.p.A., 00144 – Rome

*biancolini@ing.uniroma2.it

ABSTRACT

In this paper an innovative and fast method to tackle aeroelastic problems dealing with aircrafts is presented. This procedure is based on the use of the finite volume commercial solver ANSYS Fluent coupled with the RBF Morph tool capable to manage the structural displacement of aircraft deformable structures by properly imposing a combination of their modes through mesh morphing. Before running the FSI analysis, the modal basis of the structures is computed by means of a FEM solver and then imported into the morpher. During the CFD computing stage, these modes are combined and applied on the fly by morphing the mesh of the computational model so as to gain the deformed configuration. Mesh morphing is accomplished according to the radial basis function mathematical technique, whilst the surface aerodynamic loading is determined by performing the integration of modal forces directly on the CFD surface mesh.

The major benefit of proposed approach is that, to make the CFD model intrinsically elastic during the calculation phase, the modal parameterization has to be built only once so as to drastically reduce the computation time.

This process was applied to a real case, tested in steady flow regime conditions, with the purpose to characterize the accuracy as well as the reliability of the proposed approach. The modal approximation error was monitored and a very satisfactory agreement between numerical and experimental data was finally observed.

Keywords: Radial Basis Functions (RBF), Fluid Structure Interaction (FSI), Modal Superposition

1 INTRODUCTION

The demand for developing multi-disciplinary approach using high fidelity computer-aided engineering (CAE) methods is today strongly rising in a widespread range of technical fields including aerospace, automotive, marine, product manufacturing and healthcare to name a few. This is even more true with the vision of modern design methods which is strongly oriented to work embedded in reliable numerical optimization procedures. The core of a

multi-physics numerical investigation is the coupled-field analysis, which lets users to determine the combined effects of multiple physical phenomena as in case fluid–structure, thermal–mechanical, and electric–thermal interaction.

In particular, the fluid-structure interaction (FSI) is the interaction of movable or deformable structures with an internal or a surrounding fluid flow [1] occurring at different length scales. Such an interaction can be the working principle of the component itself (reed valves action, parachute canopy unfolding, movement of a sheet of paper within a printing device) or can be exploited to finely tune components manufacturing in view of lightening a structure as in case of aircraft design.

FSI is a typical multi-physics phenomenon which computational reproduction implies, at least, the resolution of both the structural and fluid-dynamic task and, when temperature effects are relevant, the thermal one as well. In general, the approaches to accomplish its numerical solution can be roughly grouped depending upon governing equations solution approach (monolithic and partitioned methods) and upon the treatment of meshes (conforming and non-conforming mesh methods) [2]. Besides, FSI perspectives [3] may vary depending on types of flow fields covered (such as compressible, incompressible, laminar, turbulent), types of applications, structural fields (such as thin-walled, rigid bodies, non-linear material), discretization schemes (such as finite volume, spectral methods, multi-body dynamics), flow modelling assumptions (such as continuum, statistical Lattice Boltzmann distribution) and calculation grid treatment (such as moving grid, fixed grid, immersed boundary).

Whatever the particular scenario of the study, the FSI analysis introduces a high level of complexity in the solution achievement and, as such, either the fluid forces or structural deformations are often neglected. Since in the aerodynamics sector this mechanism turns out to be crucial in many cases, both physical aspects need to be suitably accounted and, for this reason, sensible efforts have been done to this end over last decades.

One of the most delicate tasks during an FSI analysis is the movement of the computational fluid dynamic (CFD) mesh that needs to be updated in order to accommodate elastic deformations of the structure. A robust algorithm with this potential is represented by the radial basis functions (RBFs) mesh morphing, as described by the Keye' work [4] in which a complete aircraft was studied accounting for FSI in flight conditions. In the proposed approach, the method of RBFs is used for updating the CFD mesh in the deformed shape calculated by using the finite element method (FEM) modelling. Although several works [5,6,7] demonstrated that RBFs can be successfully adopted for the deformation of CFD meshes, the resulting numerical cost has limited their actual application to tackle industrial relevant cases in the past (direct solution grows by N^3 where N is the number of RBF centres). To this end, many efforts have been recently devoted to the acceleration of such a method to deal with large RBF dataset [8,9].

In order to efficiently handle aeroelastic studies through the CFD tool ANSYS[®] Fluent[®] (hereinafter referred to as Fluent), the numerical approach proposed in the present paper makes use of the RBFs technique by linking the CFD model to the RBF Morph[TM] tool. The coupling between these codes has recently proven its powerful capabilities and effectiveness by solving with success challenging engineering applications such as surface vehicle and aircraft shape design and optimisation [10,11,12], sails trim optimisation [13] and ice accretion on aircraft wings [14]. The suggested FSI numerical process fruitfully exploits the RBF Morph™ tool that enables to adapt the shape of deformable parts according to mode superposition method by smoothing mesh directly during the computing stage.

2   MODAL ANALYSIS OF DISCRETE SYSTEMS AND MODE SUPERPOSITION

The modal analysis is a well-established theory of the structural mechanics. It is applicable to both continuum and discrete systems and enables the calculation of undamped free vibration modes of a system (an object or structure), each characterized by a natural pattern (shape) and frequency.

In FEM modelling, where the behaviour of continuum systems is simulated by operating with their discrete representation, the modal analysis enables to determine the structural static and dynamic response in linearity conditions. In particular, a structure has a number of modes equal to its total number of degrees of freedom (DOF). If the damping is null and loads are not time-dependent, nodal amplitudes (modes) $\{u\}$ and natural frequencies of a structure can be computed by solving the eigenvalue problem mathematically identified by the system

$$[K]\{u\} = \omega^2[M]\{u\},$$

where $[K]$ is the stiffness matrix, ω^2 is an eigenvalue, ω is a natural frequency, and $[M]$ is the mass matrix of the system, stating that a vibration mode is a configuration in which a balance between elastic resistance and inertial loads [15] occurs.

Considering the purpose of this technique, a subset of the first modes is commonly determined and used because, since mechanical systems are characteristically low-pass, the lowest frequency modes have the highest energy levels and, then, are physically prominent. As such, the complete solution of the eigenvalue problem can be approximated retaining only a limited number of its lowest modes with a favourable reduction of DOF to be treated. Moreover, since the solution of the eigenvalue problem is a subspace of eigenvectors problem, the sign and the entity of each eigenvector may change depending on the algorithm adopted for the solution achievement [16]. Given that, for solution purposes a convenient normalization is performed by imposing for each m-th mode $\{u\}_m$ a unit modal mass so as to obtain

$$\{u\}_m^T[M]\{u\}_m = 1$$

and then

$$\{u\}_m^T[K]\{u\}_m = \omega_m^2.$$

One of most important aspects of modal analysis is the spectral decomposition, which means that modes are orthogonal and form a basis in the modal coordinates (or displacements) η [15]. In this case, the dynamic response of a mechanical system can be represented by the summation of the response of each mode. As a matter of fact, because of the orthogonality of the basis, each mode acts as a single DOF dynamic system (i.e. stiffness and mass matrixes become diagonal) and then the following system relationship is valid [16]

$$\{\ddot{\eta}\} + [\omega^2]\{\eta\} = \{N\}$$

or alternatively

$$\ddot{\eta}_m + \omega_m^2\eta_m = N_m \qquad m = 1,2,\dots,n$$

being $\ddot{\eta}_m$ and η_m respectively the nodes' acceleration and the displacement in modal coordinates, and N_m the modal force for the m-th mode.

The modal approach is usually exploited for handling dynamic analyses in which the number of retained modes is defined on the basis of excited frequencies. Nevertheless, it can be usefully employed even for approximating a static solution by superposing modes assuming the linear behaviour of the analysed system. In this specific scenario, the latter equation simplifies as follows

$$\omega_m^2\eta_m = N_m$$

and modal forces N are obtained performing the integral of the external load field over the entire structure Q weighted by the mode eigenvector $\{u\}^T$ as follows

$$N = \{u\}^T Q.$$

This latter concept means that the local force contributes to a mode if the force excites an active region (peak or valley of modal response over the space), and alternatively provides a null contribution if the force falls within an inactive region (nodal lines of the mode).

3   RADIAL BASIS FUNCTIONS

Since their inception [17], RBFs have been used as an interpolation tool of n-dimensional space scattered data, that is a mathematical means able to interpolate everywhere a scalar function defined at discrete points ensuring, at the same time, its exact value at original points. In particular, RBF methods were originated with the main purpose to overcome the too severe constraints of data treatable by numerical methods existing in the 1970s, such as the minimalism of their framework and the simplicity of the shape of their containing region. Afterwards, they experienced a very rapid development consequent to their successful application in a lot of scientific fields such as climate modelling, facial recognition, topographical map production, ocean floor mapping, and medical imaging, being resolving in many cases where polynomial interpolation failed [18].

According to a first categorization, the numerous existing RBFs can be nowadays classified on the basis of their local or global interpolation scheme and on the type of support (global or compact) they have, namely the set of points where the chosen RBF is non zero-valued [6].

In general, the solution of the RBF mathematical problem consists of calculation of the scalar parameters (sought coefficients) of the linear system of order equal to the number of considered centres [19] (source points). According to the strategy adopted by the proposed morpher tool (RBF Morph™), the RBF system solution, determined after defining a set of source points with their displacement, is employed to operate mesh morphing to the discretized domain of the computational model. Operatively, once the RBF system coefficients have been calculated, the displacement of an arbitrary node of the mesh, either inside (interpolation) or outside (extrapolation) the influence domain of source points, can be expressed as the summation of the radial contribution of each. In such a way, a desired modification of the mesh nodes position (smoothing) can be rapidly applied by preserving mesh topology in terms of total number and type of the constituting elements. As example, Figure 1 shows the localization of source nodes of the selected test case described hereafter.
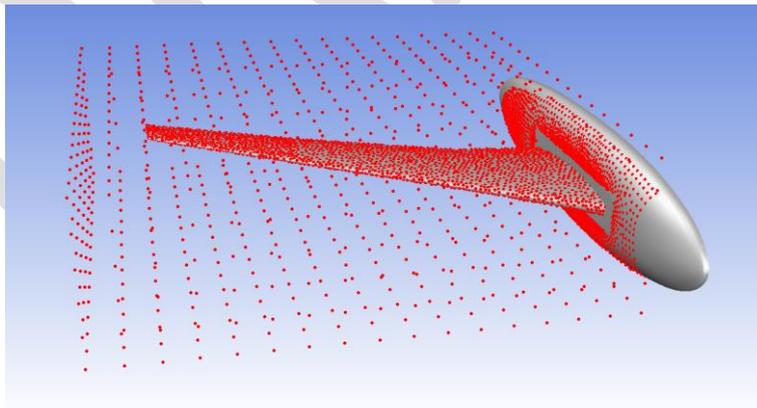

Figure 1. Source nodes for RBFs solutions generation of the test case

To afford a three-dimensional study in x, y and z coordinates, the RBF Morph™ tool utilises the RBF interpolant composed by a radial function (first term of the right side of the next equation) containing the RBF φ and a multivariate polynomial corrector vector h of order m-1, where m is said to be the order of φ, introduced with the aim to guarantee the compatibility for rigid motions. In particular, if N is the total number of introduced source points, the formulation of the RBF Morph™ interpolant is

$$s(x) = \sum_{i=1}^{N} \gamma_i \varphi\left(\|x - x_{k_i}\|\right) + h(x)$$

where x is the vector identifying the position of a generic node belonging to the surface and/or volume mesh, x_{k_i} is the i-th source node position vector, and $\|\cdot\|$ is the Euclidean norm, namely the distance between two points. The RBF fitting solution exists in case the RBF coefficients vector γ_i and the weights of the polynomial corrector vector β_i can be found such that, at source points, the interpolant function possesses the specified (known) values of displacement g_i whilst the polynomial terms give a null contribution, namely the following relations are simultaneously verified

$$s\left(x_{k_i}\right) = g_i \qquad 1 \le i \le N$$

$$\sum_{i=1}^{N} \gamma_i q\left(x_{k_i}\right) = 0$$

for all polynomials q with a degree less than or equal to that of polynomial h [6]. The minimal degree of polynomial h depends on the choice of the RBF type. It can be demonstrated that a unique RBF interpolant exists if the RBF is conditionally positive definite [20]. In the case that this latter condition is established and if the order is less than or equal to 2 [21], a linear polynomial applies

$$h(x) = \beta_1 + \beta_2 x + \beta_3 y + \beta_4 z$$

enabling to exactly recover rigid body translations.
In the event such assumptions are verified, the interpolant has the form

$$s(x) = \sum_{i=1}^{N} \gamma_i \varphi\left(\|x - x_{k_i}\|\right) + \beta_1 + \beta_2 x + \beta_3 y + \beta_4 z$$

and γi and βi values can be obtained by solving the system

$$\begin{pmatrix} M & P \\ P^T & 0 \end{pmatrix} \begin{pmatrix} \gamma \\ \beta \end{pmatrix} = \begin{pmatrix} g \\ 0 \end{pmatrix}$$

where M is the interpolation matrix having the elements derived by calculating all the radial interactions between source points as follows

$$M_{ij} = \varphi\left(\left\|x_{k_i} - x_{k_j}\right\|\right) \qquad 1 \le i \le N, \qquad 1 \le j \le N,$$

and P is a constraint matrix that arises balancing the polynomial contribution containing a column of 1 and the spatial positions of source points in the remaining three columns, that is

$$P = \begin{pmatrix} 1 & x_{k_1} & y_{k_1} & z_{k_1} \\ 1 & x_{k_2} & y_{k_2} & z_{k_2} \\ \vdots & \vdots & \vdots & \vdots \\ 1 & x_{k_N} & y_{k_N} & z_{k_N} \end{pmatrix},$$

assuming that source points are not contained in the same plane (otherwise the interpolation matrix would be singular).
For what described, by satisfying the displacement field prescribed at source points, RBF Morph™ operates the smoothing of mesh nodes using the following formulation of the interpolant

$$\begin{cases} s_x(\boldsymbol{x}) = \sum_{i=1}^{N} \gamma_i^x \varphi(\|\boldsymbol{x} - \boldsymbol{x_{k_i}}\|) + \beta_1^x + \beta_2^x x + \beta_3^x y + \beta_4^x z \\[2mm] s_y(\boldsymbol{x}) = \sum_{i=1}^{N} \gamma_i^y \varphi(\|\boldsymbol{x} - \boldsymbol{x_{k_i}}\|) + \beta_1^y + \beta_2^y x + \beta_3^y y + \beta_4^y z \\[2mm] s_z(\boldsymbol{x}) = \sum_{i=1}^{N} \gamma_i^z \varphi(\|\boldsymbol{x} - \boldsymbol{x_{k_i}}\|) + \beta_1^z + \beta_2^z x + \beta_3^z y + \beta_4^z z \, . \end{cases}$$

In the end, RBF methods have shown several advantages that make them very attractive in the area of mesh smoothing. One of the most important is that, because of their meshless scheme, only the grid points are moved regardless of the volume cells they belong to, as well as regardless of specific key features that can be involved in smoothing such as, for instance, non-conformal interfaces.

Furthermore, they also are particularly suitable for parallel implementation and so potentially able to manage huge cases. As a matter of fact, once RBF solutions are known and shared in memory, each calculation process working on a mesh partition has the ability to smooth its nodes without taking care of what happens outside, because the smoother is a global point function and the continuity at interfaces is then implicitly guaranteed. As an example Cella & Biancolini [12] stressed the RBF solver using a set-up of about 430.000 points to morph a 14 million hexahedrons mesh that means about 14 million of nodes. It takes 1337 s to fit and 5445 s to morph on a quadcore.

4   DESCRIPTION OF THE PROPOSED NUMERICAL ANALYSIS STRATEGY

The workflow of the proposed approach conceived to handle FSI numerical studies is composed by the following sequential three stages (Figure 2):
Stage1: modes calculation (FEM solver).
Stage2: RBF solutions generation and storing (RBF Morph™).
Stage3: FSI computing using the CFD flexible model embedding RBF solutions (Fluent coupled with RBF Morph™).

In Stage1, structural modes of deformable parts are calculated and extracted by means of a FEM model. To achieve an effective coupling in Stage3, this model has to be defined using position orientation and units compatible with the CFD one. As a consequence, the starting geometry, if any, has to be the same also in the event different mesh spacing is adopted because the RBF approach is meshless [22]. Generally speaking, in fact, the CFD model requires a refinement of the wetted surfaces finer than the FEM one, and then these meshes are typically not conformal for relevant industrial applications. As such, an interpolation is required for exchanging information that, for standard aeroelastic coupling, is bi-directional in the sense that pressure distribution computed through CFD have to be mapped onto the FEM mesh, whilst deformations calculated through FEM have to be used to update CFD surface shapes adjusting the volume mesh accordingly.
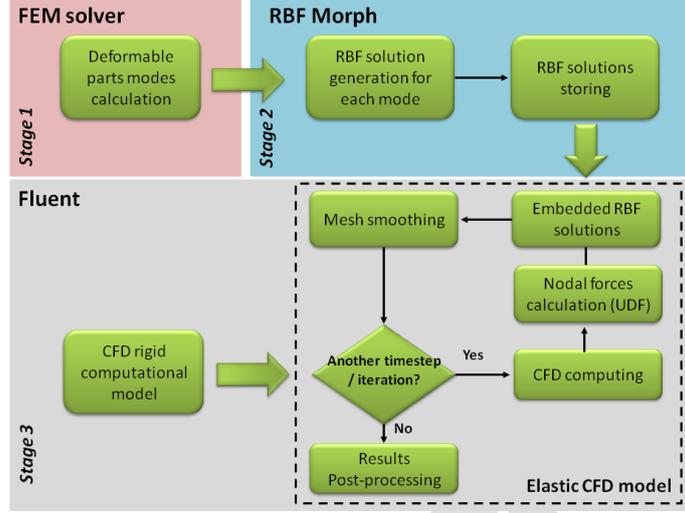
Figure 2. Workflow of the FSI proposed approach

In Stage2 the morphing problem is fully defined, namely the RBF solution is calculated for each mode by applying to the deformable surfaces the displacements of the corresponding mode gained through the FEM model, and constraining the surfaces considered behaving as rigid by imposing a zero motion. Since an adequate level of mesh quality after smoothing is required by the CFD solver, some of RBF Morph™ parameters and features, such as source point's density and dimensions of the domain interested by the morphing action, shall have to be properly tuned. Once calculated, all RBF solutions are stored and ready to be embedded in the CFD model.

In Stage3 the FSI coupling is enabled. The stored RBF solutions are loaded once at the beginning of the step so as making elastic the CFD model , that is capable to adapt its shape when loaded. As concerns mesh updating, a proper scheduling needs to be carefully considered because on the one hand mesh updating introduces a small numerical noise and, on the other hand, it is not required at every iteration (steady analysis) or timestep (unsteady analysis).

This crucial operation is straightforward executed because the structural response is evaluated directly in the modal space according to the following relation

$$X_{CFD} = X_{CFD0} + \sum_{m=1}^{n_{modes}} \eta_m \delta X_m$$

where X_{CFD0} are the position of CFD nodes of undeformed mesh (baseline configuration), η_m are the (unknown) values of modal coordinates and δX_m are the modal displacements for the generic retained m-th mode. Since according to the proposed approach CFD forces are demanded, they are evaluated using nodal conversion instead of employing the standard flow loading mapping. This operation allows to avoid the high-demanding efforts related to mapping and it is straightforwardly accomplished by means of Fluent user defined functions (UDFs). In detail, a loop over all faces to calculate the resulting force accumulated at each node is performed by taking into account the contribution coming from each connected face, assuming an uniform value on one single face. For what just described, modal forces N_m are calculated as follows

$$N_m = \sum_{i=1}^{n_{surf}} \delta X_{m_i}{}^T F_i$$

7

where the m-th modal load is a scalar obtained summing the dot product between nodal load and nodal mode displacement of each i node of n_{surf} nodes of the surface. Considering that a mass normalization criterion was defined for modes extraction, the modal coordinates are

$$\eta_m = \frac{N_m}{\omega_m{}^2}$$

and the parametric CFD mesh can adapt its shape on the basis of actual loads according to the following relationship

$$X_{CFD} = X_{CFD0} + \sum_{m=1}^{n_{modes}} \frac{N_m}{\omega_m^2} \delta X_m.$$

It is worth mentioning that, since FEM results are transferred onto a set of CFD model surfaces adopting a multiple local problem scheme, the pressure loading coming from different areas can be managed separately if required. Such an approach allows to efficiently handle important FSI applications where relative sliding motion among parts of wetted surfaces occurs.

Besides, the whole approach is general in the sense that it can be also applied to unsteady analyses modifying the time scheduling for smoothing application.

5   TEST CASE

To showcase the effectiveness and efficiency of the proposed technique in solving real world aircraft FSI applications, one of the configurations of the Aeroelastic Prediction Workshop [23] (AePW), launched with the main purpose to assess the capability of the most advanced numerical methods in predicting static and dynamic aeroelastic phenomena and responses, was simulated. In particular, the test case of interest is referred to as HIgh REynolds Number Aero-Structural Dynamics [24] (HIRENASD) and consisted of a tapered 34 degrees aft-swept wing with a BAC3-11/RES/30/21 supercritical airfoil profile specifically designed to achieve high structural stiffness and distant modes on frequency domain. The real model, shown in Figure 3, was tested in the Cologne European Transonic Wind tunnel (ETW) for a Mach number ranging from 0.8 to 0.88.

Figure 3. HIRENASD wind tunnel model

In order to carry out all the afore-described steps of the FSI study, FEM and CFD grids as well as the testing parameters, provided to support AePW participants, were employed.

In the view of obtaining the modal basis, a tetrahedral FEM model of the assembly defined by the wing, the excitation system and the balance was adopted, and the first six mass normalized modes were extracted using NX Nastran. Wing modal shapes and their respective frequencies are shown in Figure 4 (horizontal view), where B and FA respectively stand for out-of-plane bending and in-plane fore-and-aft bending according to AePW mode classification.

Mode 1 – 1B - 25.5 Hz   Mode 2 – 2B - 80.2 Hz   Mode 3 – 1FA - 106.1Hz

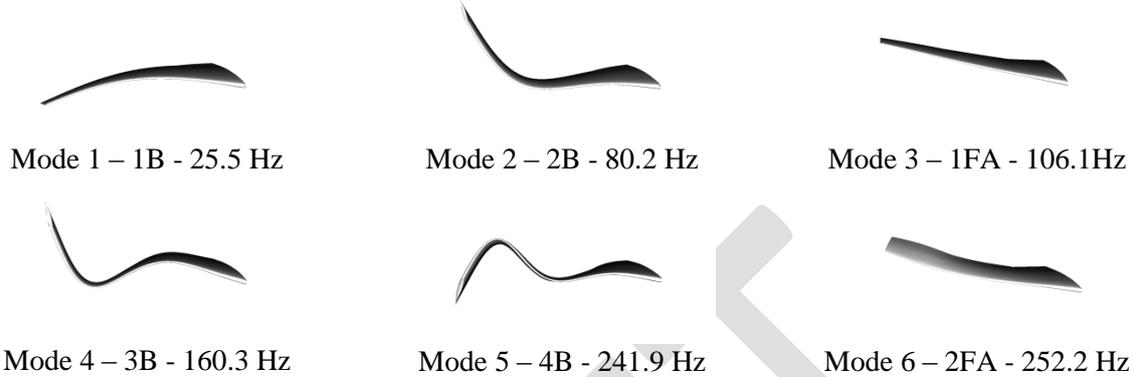Mode 4 – 3B - 160.3 Hz   Mode 5 – 4B - 241.9 Hz   Mode 6 – 2FA - 252.2 Hz

Figure 4. Mode number, description, frequencies and modal shapes for the HIRENASD FEM model

FEM grid nodal displacements of modal shapes were applied to the wing CFD surface mesh of the CFD model through RBF Morph™ utilizing results data exported according to Nastran format. Moreover, since in both the wind tunnel and the FEM model the fuselage aerodynamic fairing is mechanically uncoupled from the wing root so that a slight motion of the wing root is allowed, a small portion of the fuselage around the wing of the CFD model was left free to deform using a buffer so as to absorb the required motion. Figure 5 depicts the CFD model morphed according to the mode 2 superposed to the baseline configuration. The image clearly evidences the buffer around the wing root as well as the box-shaped encapsulation domain [25] suitably generated to limit the morphing action. The total number of source nodes of the optimized set-up was about 4500.
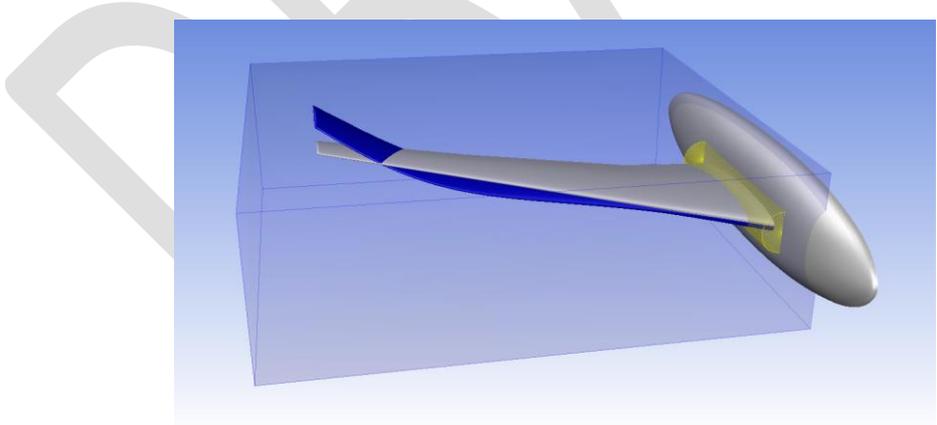
Figure 5. Morphed configuration corresponding to structural mode 2

The FSI computing was divided in two subsequent simulation phases that ran on a mixed 1.5 million cell SOLAR unstructured grid made available by German Aerospace Center (DLR) and The National Aeronautics and Space Administration (NASA). In particular, at first a conventional CFD simulation was carried out using the stiff model to gain a fully developed field, whereas in a second phase the elastic behaviour of the model was finally taken into account by embedding the RBF solutions (see Figure 2). This strategy was adopted to

accelerate the CFD convergence in the second phase since the initial CFD field for the flexible computing was realistically supposed not to be far from the final one.

The FSI analysis parameters proposed by AePW were 0.8 Mach with a $7 \cdot 10^6$ Reynolds number based on the 0.3445 m reference chord. To reach the required Reynolds number, as suggested in the reference workshop, the simulation was carried out using Nitrogen at 136180 Pa and 278.5 K as test medium. Given the transonic condition of the problem, a steady pressure based implicit solver was utilized with the roe-FDS flux scheme, using the Green-Gauss node based spatial discretization for the gradient and the second order upwind scheme as a test medium for the flow and the modified turbulent viscosity. The Spalart Allmaras single equation model was applied for turbulence and the pressure far-field boundary condition was imposed to the hemispheric patch enclosing the symmetric calculation domain. On wing and fuselage surfaces a no-slip condition was set. The model simulated a 1.5 degrees angle of attack (AoA). The direct integration of modal forces on the CFD mesh and the mesh updating process were invoked every 25 iterations (setting-up a calculation activity feature of Fluent), and throughout the simulation aerodynamic coefficients and the position of sensible nodes on wing were monitored and stored for validation purposes.

In order to obtain a preliminary judgment of the accuracy of results obtained through modal superposition, the maximum displacement of wing at tip, calculated through up to 6 modes, was compared to the one achieved using a full two-way coupling envisaging the use of data mapping (Table 1). The achieved results evidence how each added mode reduces the error improving the matching with the reference deformed shape obtained by full two-way coupling. The lowest achievable error was registered once having included up to four modes.

Number of modes	Maximum wing displacement (mm)	Relative error (%)
1	15.26	-5.64
2	14.18	1.81
3	14.18	1.80
4	14.26	1.29
5	14.26	1.29
6	14.26	1.29
Full two-way approach (mapping)	14.44	-

Table 1. Basis validation of the first 6 modes with respect to mapping

Convergence with the CFD elastic model was reached after only 5 mesh updating iterations using the first 6 modes mainly to minimize the error. A final displacement of 0.01274 m was obtained. This result is in good agreement with the 0.0125 m displacement evidenced by experimental data [26].

In Table 2 the strong influence of the elastic behavior in aerodynamic coefficients evaluation is shown by taking into account the rigid and elastic model responses. Lift and drag coefficients computed using the proposed approach are favorably compared to literature numerical values [26].

Aerodynamic coefficient	Rigid model		Elastic model	
	Proposed model	NASA model	Proposed model	NASA model
C_l	0.3572	0.3542	0.3403	0.3373
C_d	0.0167	0.0173	0.0160	0.0166
C_m	-0.5596	-0.5516	-0.5307	-0.5231

Table 2. Comparison of numerical obtained aerodynamic coefficients

In Figure 6 the pressure coefficient distribution obtained at different sections on the CFD elastic model is plotted in conjunction with the corresponding value measured by experiments and available in literature [26]. Specifically, from left to right and from top to bottom, these sections refer respectively to wing span ξ equal to 14.5% (Section 1), 32.3% (Section 2), 65.5% (Section 5) and 95.3% (Section 7). As evident, data alignment turns out to be very satisfying.

Section 1   Section 2

Section 5   Section 7
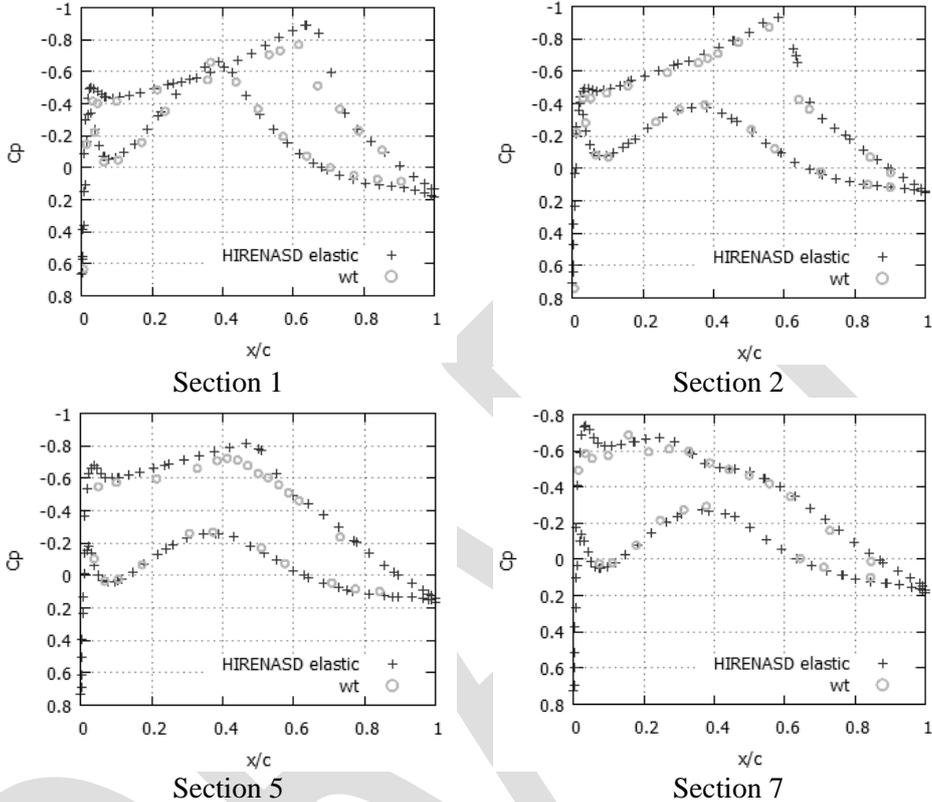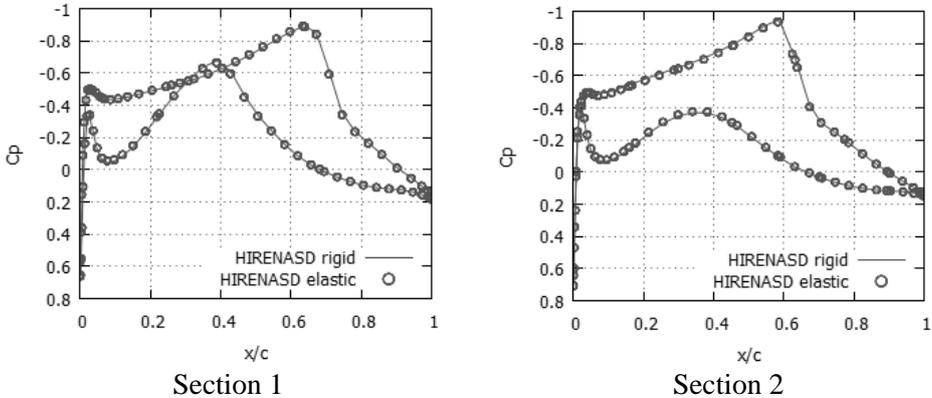
Figure 6. Comparison between numerical and experimental data at different wing sections

The pressure coefficient values computed at the same sections of the previous figure by means of the rigid and elastic model, plotted respectively through a continuous trait and circles, are illustrated in Figure 7.

Section 1   Section 2

11

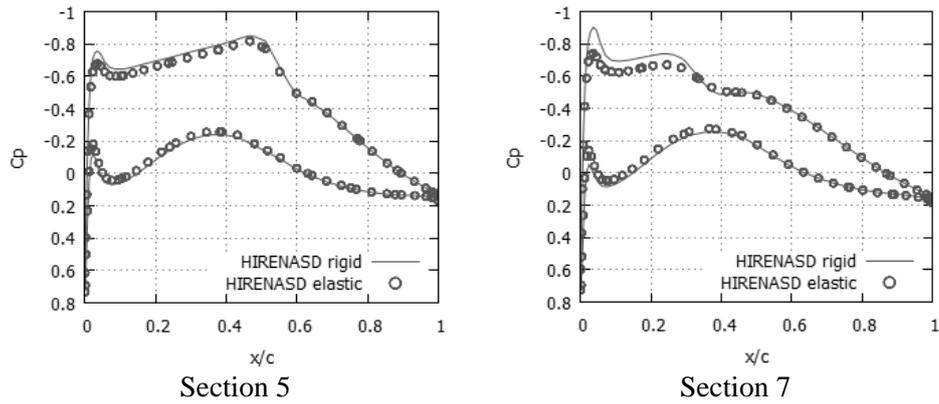<div align="center">Section 5   Section 7</div>

Figure 7. Pressure coefficients for the rigid and the elastic HIRENASD model at different span sections.

These results highlight the importance of an aeroelastic analysis especially for the outer sections of the wing, where the alteration introduced by elasticity cannot be neglected.

The whole Fluent simulation was completed in 876 iterations, whose most part (780 iterations) were performed using the rigid model whilst the flexible model experienced the wing shape updating for four times. For what described, the actual aeroelastic simulation took only 96 iterations to converge, meaning that the proposed approach allows fulfilling a FSI calculation with a computational cost comparable with that of a rigid one.

6   CONCLUDING REMARKS

An aeroelastic numerical procedure to efficiently and reliably simulate real world aircraft FSI applications was proposed and described. In order to validate this novel calculation procedure, a well-tested wind tunnel case was simulated in transonic flow conditions and the results obtained by numerical modelling have been favourably compared to those measured during the referenced experimental campaign.

The added value offered by the proposed technique is its ability to make flexible the Fluent computational model embedding the structural modes of deformable parts preventively calculated using a FEM tool code by means of the RBF Morph™ tool.

Indeed, this latter technique easily couples the modes shape to the mesh of the computational grid (surface and volume) by a smoothing action. The main advantage with respect to other standard approaches is that the modal parameterization has to be built only once. The final result is that the new CFD model becomes intrinsically elastic during the calculation stage.

Finally, the proposed FSI approach can be suitably applied to both steady and unsteady aeroelastic studies and its use can be extended to very large models where RBF Morph™ has already proven its computational time efficiency.

REFERENCES

[1]   H.J. Bungartz, M. Schäfer, Fluid-structure Interaction: Modelling, Simulation, Optimization (2006), Springer-Verlag.

[2]   H. Gene, W. Jin, L. Anita, Numerical Methods for Fluid-Structure Interaction - A Review, Commun. Comput. Phys. (2012), Vol. 12, No. 2, pp. 337-377.

[3]   E. Costa, Advanced FSI analysis within ANSYS Fluent by means of a UDF implemented explicit large displacements FEM solver (2012), Ph.D. Program in Environment and Energy - Cycle XXIV, Industrial Engineering Department of the University of Rome Tor Vergata.

[4]   S. Keye, "Fluid-structure coupled analysis of a transport aircraft and comparison to flight data," 39th AIAA Fluid Dynamics Conference AIAA-2009-4198.

[5]   S. Jakobsson, O. Amoignon, "Mesh deformation using radial basis functions for gradient based aerodynamic shape optimization," Computers and Fluids Vol. 36, Iss. 6, July, 2007, pp. 1119-1136.

[6]   A. de Boer, M.S. van der Schoot, H. Bijl, "Mesh deformation based on radial basis function interpolation," Computers and Structures Vol. 85, Iss. 11-14, June - July, 2007, pp. 784-795.

[7]   van Zuijlen, A.H., de Boer, A., Bijl, H., "Higher-order time integration through smooth mesh deformation for 3D fluid–structure interaction simulations," Journal of Computational Physics Vol. 224, 2007, pp. 414–430.

[8]   Rendall, T.C.S., Allen, C.B. (2009). Efficient Mesh Motion using Radial Basis Functions with Data Reduction Algorithms, Journal of Computational Physics, 228, 6231–6249

[9]   Rendall, T.C.S., Allen, C.B. (2010). Reduced Surface Point Selection Options for Efficient Mesh Deformation Using Radial Basis Functions, Journal of Computational Physics, 229, 2810–2820.

[10]   S. Sovani, A. Khondge, Scaling New Heights in Aerodynamics Optimization: The 50:50:50 Method (2012), ANSYS White paper.

[11]   M.E. Biancolini, E. Costa, F. Lagasco, J. Dariva, U. Cella, M. Mancini, G. Travostino, Tecniche di Mesh Morphing per l'ottimizzazione in campo aeronautico, Analisi e Calcolo, Numero 56, Maggio 2013.

[12]   U. Cella, M.E. Biancolini, Aeroelastic Analysis of Aircraft Wind-Tunnel Model Coupling Structural and Fluid Dynamic Codes (2012), Journal of Aircraft Vol. 49, No. 2.

[13]   M.E. Biancolini, I.M. Viola, M. Riotte, Sails trim optimisation using CFD and RBF mesh morphing, Computers and Fluids, Elsevier (under revision).

[14]   M.E. Biancolini, C. Groth, Use of RBF mesh morphing for the estimation of aerofoil performances in presence of ice profiles (2013), UGM ANSYS Italia 2013 Proceedings.

[15]   R.D. Cook, D.S. Malkus, M.E. Plesha, R.J. Witt, Concepts and Applications of Finite Element Analysis, 4th Edition (2002), John Wiley & Sons.

[16]   L. Meirovitch, Fundamentals of Vibrations (2010), Aveland Pr Inc, Reissue edition.

[17]   R.L. Hardy, Multiquadric equations of topography and other irregular surfaces, Journal of Geophysical Research 76 (1971), no. 8, 1905–1915.

[18]   S.A. Sarra, Radial basis function approximation methods with extended precision floating point arithmetic, Engineering Analysis with Boundary Elements 35 (2011), no. 1, 68–76.

[19]   M.D. Buhmann. Radial Basis Functions (2003), Cambridge University Press, New York, NY, USA.

[20]   C. Micchelli, Interpolation of scattered data: Distance matrices and conditionally positive definite functions, Constructive Approximation 2 (1986), 1122.

[21] A. Beckert, H. Wendland, Multivariate interpolation for fluid-structure-interaction problems using radial basis functions, Aerospace Science and Technology (2011), Volume 5, Issue 2, Pages 125-134, ISSN 1270-9638.

[22] M.E. Biancolini, Mesh Morphing and Smoothing by Means of Radial Basis Functions (RBF): A Practical Example Using Fluent and RBF Morph, Handbook of Research on Computational Science and Engineering: Theory and Practice, 2 vol. pages 347-380, 2012.

[23] https://c3.nasa.gov/dashlink/projects/47/

[24] http://heinrich.lufmech.rwth-aachen.de/en

[25] RBF Morph, RBF Morph - Users' Guide (2012).

[26] P. Chwalowski, , J.P. Florance, , J. Heeg, C.D. Wieseman, and B. Perry, Preliminary computational analysis of the HIRENASD configuration in preparation for the aeroelastic prediction workshop (2011), IFASD-2011-108 (2013) 1–21.